Picosecond pulse amplification up to a peak power of 42W by a quantum-dot tapered optical amplifier and a mode-locked laser emitting at 126 µm

Picosecond pulse amplification up to a peak power of 42 W by a quantum-dot tapered optical amplifier and a mode-locked laser emitting at 1.26 μm

Christoph Weber,[1] Lukas Drzewietzki,[1] Mattia Rossetti,[2] Tianhong Xu,[2] Paolo Bardella,[2] Hercules Simos,[3] Charis Mesaritakis,[3] Mike Ruiz,[4] Igor Krestnikov,[5] Daniil Livshits,[5] Michel Krakowski,[4] Dimitris Syvridis,[3] Ivo Montrosset,[2] Edik U. Rafailov,[6] Wolfgang Elsäßer,[1] and Stefan Breuer[1,*]

[1]*Institute for Applied Physics, Technische Universität Darmstadt, Schlossgartenstr. 7, 64289 Darmstadt, Germany*

[2]*Dipartimento di Elettronica e Telecommunicazioni, Politecnico di Torino, Corso Duca degli Abruzzi 24, 10129 Torino, Italy*

[3]*National and Kapodistrian University of Athens, Panepistimiopolis, Ilissia, Athens 15784, Greece*

[4]*Alcatel-Thales-III-V Lab, Route Départementale 128, 91767 Palaiseau Cedex, France*

[5]*Innolume GmbH, Konrad-Adenauer-Allee 11, 44263 Dortmund, Germany*

[6]*Institute of Photonic Technologies, Aston University, Birmingham B4 7ET, UK*

**Corresponding author: stefan.breuer@physik.tu-darmstadt.de*

Received October 16, 2014; revised December 18, 2014; accepted December 22, 2014; posted December 23, 2014 (Doc. ID 225040); published January 29, 2015

We experimentally study the generation and amplification of stable picosecond-short optical pulses by a master oscillator power-amplifier configuration consisting of a monolithic quantum-dot-based gain-guided tapered laser and amplifier emitting at 1.26 μm without pulse compression, external cavity, gain- or *Q*-switched operation. We report a peak power of 42 W and a figure-of-merit for second-order nonlinear imaging of 38.5 W^2 at a repetition rate of 16 GHz and an associated pulse width of 1.37 ps. © 2015 Optical Society of America

OCIS codes: (140.5960) Semiconductor lasers; (250.5980) Semiconductor optical amplifiers; (140.3538) Lasers, pulsed; (250.5590) Quantum-well, -wire and -dot devices; (140.2020) Diode lasers; (140.4050) Mode-locked lasers.
http://dx.doi.org/10.1364/OL.40.000395

Stable short optical pulses with high peak power at near-infrared wavelengths are essential in nonlinear biomedical imaging modalities including two-photon excitation fluorescence microscopy (TPEF) or second-harmonic imaging microscopy. In particular, excitation wavelengths in the 1.3 μm region are promising due to a high penetration depth into organic tissue [1]. Nowadays, solid-state Ti:sapphire-lasers with optical parametric oscillators are the dominant pulsed excitation laser sources for second-order nonlinear imaging including TPEF in this wavelength region. However, besides their ultra-short pulses, high optical peak power, and broad wavelength tuning range, they are still bulky, complex and expensive. The suitability of a pulsed laser for nonlinear imaging can be quantified by a figure-of-merit (FOM) that is defined by the product of squared peak power times the duty cycle, thus being a measure for the generated TPEF signal [2]. Much simpler and robust pulsed all-semiconductor laser systems have already demonstrated exceptionally high pulse peak power and FOM of 100 W and 27 W^2, respectively, at a wavelength of 800 nm [3], 366 W (311 W^2) at 922 nm [4], 1.4 kW (271 W^2) at 975 nm [5], 2.5 kW (1281 W^2) at 830 nm [6], and 6.5 kW (5233 W^2) at 850 nm [7]. All systems use an external-cavity configuration and employ, except of [3], pulse post-compression techniques. Without pulse compression and at wavelengths above 1 μm, a peak power of 65 W at 1.063 μm and 35-ps short pulses have been reported for a gain-switched three-section laser and post-amplification by a two-section semiconductor optical amplifier (SOA) with electrically pulsed flared gain section resulting in a FOM of 0.15 W^2 [8]. A comparable peak power of 50 W at 1.066 μm and pulse width of 80 ps and a FOM of 0.25 W^2 have been reported for *Q*-switching when the absorber section of the three-section laser is electrically modulated [9]. A peak power of 2.7 W at 1.55 μm and a pulse width of 100 ps leading to a FOM of 0.73 W^2 have been reported by a tapered laser with a distributed-feedback (DFB) master oscillator [10]. An increased FOM of 3.12 W^2 has been reported at 1.06 μm with a peak power of 6.3 W and 74 ps short pulses by gain-switching of a three-section laser consisting of a straight DBR section, a straight absorber section and a flared gain section [11]. By gain-switching a single-section straight DFB laser followed by a two-section SOA with a straight and a flared section, 23-W peak power at 1.063 μm with pulse widths of 40 ps and a FOM of 3.68 W^2 have been realized [12]. Compact InAs/InGaAs quantum dot (QD) lasers are ideal alternative pulsed sources due to their ultra-fast gain and absorption dynamics, broad tunable wavelength range, and emission wavelengths in the desired wavelength region of 1.3 μm [13,14]. With pulse compression and at 1.3 μm, 290-fs short pulses and 0.34-W peak power with a FOM of 34 μW^2 have been reported using a hybrid mode-locked external-cavity two-section InGaAs quantum-dot (QD) laser with postamplification [15]. At 1.3 μm, a peak power of 0.5 W with 780-fs short pulses and a FOM of 5 mW^2 have been obtained for a single-chip two-section QD laser with tapered gain section [16]. An external-cavity QD laser with post-amplification by a QD-SOA has been reported at 1.26 μm yielding a peak power of 26 W and a pulse width of 16 ps, thus leading to a FOM value of 7.7 W^2 [17].

In this Letter, we experimentally study the generation and amplification of stable and nearly transform-limited picosecond pulses at 1.26 μm with high peak power and FOM generated by a simple all-QD master oscillator

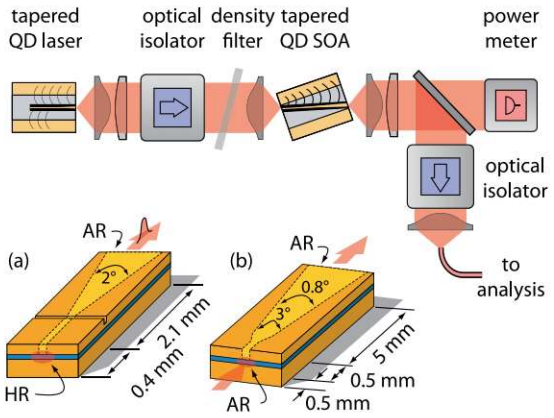

Fig. 1. Schematic of the MOPA setup and geometries of the (a) tapered QD laser and (b) the tapered QD SOA.

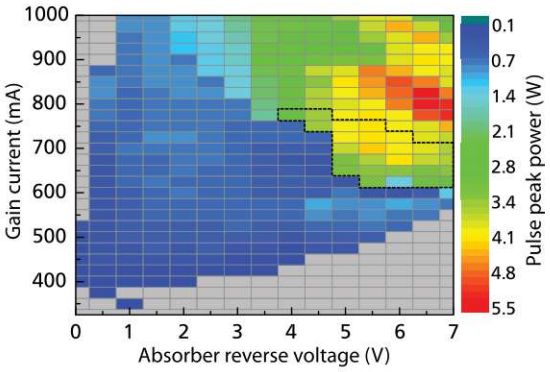

Fig. 2. Dependence of laser pulse peak power on laser current and absorber reverse-bias voltage. The area within the dashed boundary indicates stable pulse generation.

power amplifier (MOPA) without pulse post-compression. A schematic of the realized QD MOPA setup is depicted in Fig. 1 together with the geometries of the developed tapered two-section QD laser and tapered SOA. Both device designs have been optimized by numerical simulations for high-power short-pulse generation and amplification [18,19]. Both active regions of the laser and amplifier consist of 10 layers of InAs/InGaAs QDs. The light field in both of the devices is gain-guided with an additional weak index-guiding of the light field in the SOA for a better lateral confinement. The 400-μm-long absorber section of the two-section laser is biased with a negative voltage to achieve nonlinear absorption, while the tapered section is forward biased to provide gain both leading to mode-locked operation. The absorber section end facet is high-reflective coated, while the emission facet is anti-reflective coated. The tapered SOA consists of one straight input section and two additional subsequent tapered gain sections leading to a total amplifier length of 6 mm. The purpose of the straight section is to improve input coupling, while the tapered gain sections provide main amplification. Both SOA facets are anti-reflective coated and are tilted with respect to the waveguide to minimize back-reflections. While the laser temperature is kept at 20°C, the SOA is cooled to 14°C to realize ideal matching of laser emission wavelength and central gain wavelength of the SOA. We assume an input coupling efficiency of the laser light to the SOA of around 20%. Using a *tapered* master oscillator offers the potential of a high power reserve, thus no preamplifier is necessary, and input coupling optimization is not vital. An estimation of the saturation input power of the SOA is difficult as the input coupling is not known precisely. In the MOPA schematic in Fig. 1, the light from the laser is first collimated using an aspheric lens and a cylindrical lens, attenuated and focused into the SOA using an aspheric lens. The free-space guiding in combination with the lenses allows for a good mode-matching of laser and SOA. In addition, pulse broadening due to fiber dispersion is prevented. The amplified light is collimated by a combination of an aspheric and a cylindrical lens, fiber coupled, and directed to an optical spectrum analyzer (OSA) to determine the spectral shape and width as well as to an intensity auto-correlator to determine the pulse shape and pulse width. The average power is measured free-space using an optical power meter. The pulse repetition frequency and stability is quantified with a high-speed photo-detector coupled to a radio-frequency spectrum analyzer. Optical isolators between laser and amplifier and additionally in front of the fiber coupling prevent destabilizing and parasitic optical feedback into the laser. Prior to the pulse amplification, we verify stable pulse generation with high peak power. The resulting dependence of pulse peak power on laser current and absorber reverse-bias voltage is depicted in Fig. 2. The area indicated by the dashed boundary denotes the region of stable pulse generation. Stability was determined by the existence of a clean and narrow Lorentzian-shaped beat signal of the mode-locked laser as well as the absence of any other signals in the electrical spectrum. For the amplification measurements, the laser is operated at a current of 649 mA and at a reverse bias of 6 V. For this operating condition, stable short optical pulses without Q-switched mode-locking (ML) or modulation instabilities are obtained as indicated in Fig. 3. The fundamental repetition frequency of the laser at 16 GHz is depicted with a Lorentzian fit and, as the inset, a full-span view of the electrical spectrum. A Lorentzian line-width of 17.6 kHz indicates an excellent ML stability in general and a low pulse-to-pulse timing jitter of only 26 fs. Sidebands visible in the full-span-spectrum, inset of Fig. 3, originate from weak amplitude

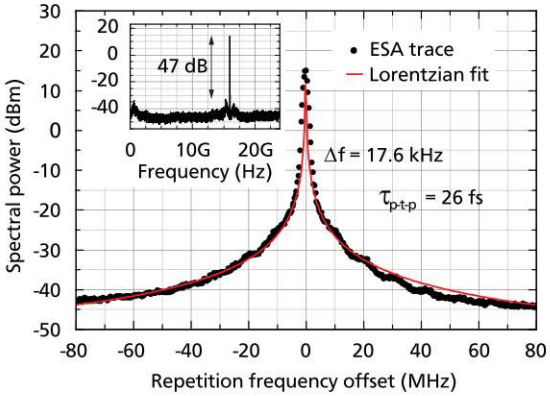

Fig. 3. Electrical spectrum of the mode-locking beat of the laser at a current of 649 mA and at a reverse bias of 6 V. The Lorentzian fit allows to estimate the width Δf of the beat signal. Inset: full-span RF spectrum.

modulations but are suppressed with a high signal-to-noise ratio of over 47 dB and therefore are negligible. The deconvoluted pulse width of the laser amounts to 1.2 ps using a Gaussian fit. The laser emission exhibits a full-width divergence angle ($1/e^2$) of the slow axis of 3.1°. M^2 is estimated to be 1.7 for a gain current of 675 mA and a reverse bias of −6 V (Laser A in [20]). Simulations suggest an M^2 value of 3 for the SOA [19]. To considerably increase the peak power of the monolithic laser, we investigate the pulse amplification for high SOA gain currents of up to 7 A. Before focusing the laser output into the SOA, the average output power of the laser is attenuated to 6 mW to avoid early gain saturation of the SOA. The left inset in Fig. 4 depicts an exemplary optical spectrum of the amplified pulses and indicates both the very broad ASE from the SOA and the amplified coherent signal. In order to determine the amount of usable amplified coherent output power, we quantify the amplified spontaneous emission (ASE) from the SOA output after amplification by evaluation of the optical spectrum. We identify and calculate the coherent part of the optical spectrum after amplification. We first integrate the whole optical power in the spectrum and subtract the ASE part, determined by connecting the ASE parts in the spectrum by a linear interpolation, as depicted. The ratio of this difference and the whole integrated spectrum is multiplied with the total SOA output power to obtain the usable coherent output power. The distinct shape of the amplified spectrum indicates self-phase modulation of the pulses in the SOA [21]. By this approach, the coherent average SOA output power is obtained, which is depicted in Fig. 4. A nearly linear increase of average power as a function of SOA current is found without signs of saturation. The pulse widths obtained after amplification are depicted in Fig. 5 and result from fitting the auto-correlator time traces with a well-matching Gaussian function as exemplarily depicted in the right inset of Fig. 4. The noise level of 2.5 stems from stray light within the auto-correlator. The pulse peak power P_{peak} after pulse amplification is calculated by $P_{\mathrm{peak}} = P_{\mathrm{avg}} f_{\mathrm{psf}}/(f_{\mathrm{rep}}\Delta t)$ with the average

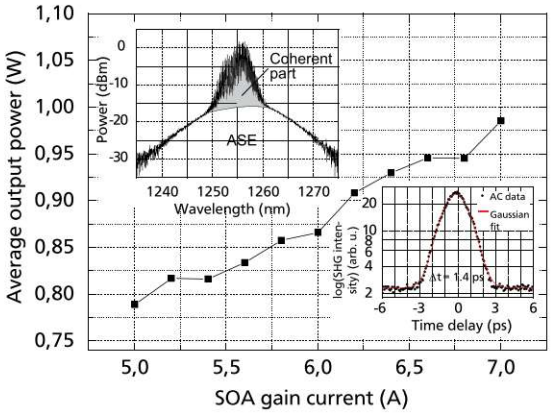

Fig. 4. Coherent average output power of the amplified pulses as a function of the SOA injection current. Left inset: typical optical spectrum of the amplified pulses at a SOA current of 5.4 A. Right inset: intensity auto-correlation time trace of the amplified pulses at a SOA current of 7 A. The Gaussian fit indicates a deconvoluted pulse width of 1.37 ps.

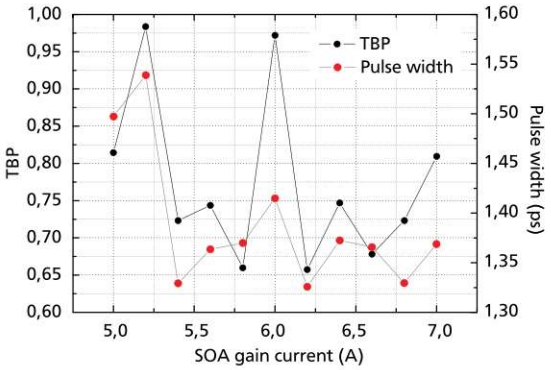

Fig. 5. Pulse width (right scale) and TBP (left scale) of the amplified pulses as a function of the SOA gain current.

power P_{avg}, the pulse repetition rate f_{rep}, the deconvoluted pulse width Δt, and the pulse shape factor (PSF) $f_{\mathrm{psf}} = 0.94$. The pulse shape factor is necessary to obtain the correct peak power as it accounts for the energy inside the temporal wings of the pulse according to $f_{\mathrm{psf}} = B \cdot H/A$ with B being the width, H the height, and A the area of the assumed pulse shape. Consequently, the FOM is thus given by $\mathrm{FOM} = P_{\mathrm{avg}}^2 f_{\mathrm{psf}}^2/(f_{\mathrm{rep}}\Delta t)$. The FOM and peak power values referred to in the introduction were calculated omitting the PSF. The measured pulse width and the time–bandwidth product (TBP) are depicted in Fig. 5. The minimum TBP of 0.66 at 6.2 A indicates only weak chirp. In general, the TBP correlates with the pulse width. The minimum pulse width amounts to 1.33 ps at 6.2 A. The relatively low TBP of 0.80 at the highest applied SOA current of 7 A obviates the use of post-compression because a typical dual-grating-based compressor exhibits transmission losses of at least 50%. The estimated pulse peak power is shown in Fig. 6 displaying a maximum value of 42 W with a pulse width of 1.37 ps for the highest applied SOA gain current of 7 A. Even though the amplified pulse widths are larger than the pulses of the laser, a broadening trend to higher amplification currents is not observed (Fig. 5) thus giving the potential to a steady peak power increase by increasing the amplification current. Due to such high peak powers and the high repetition rates, the achieved FOM, which is depicted in Fig. 6, reaches a value of 38.5 W^2 well exceeding state-of-the-art results for mode-locked lasers with post-amplification and without pulse

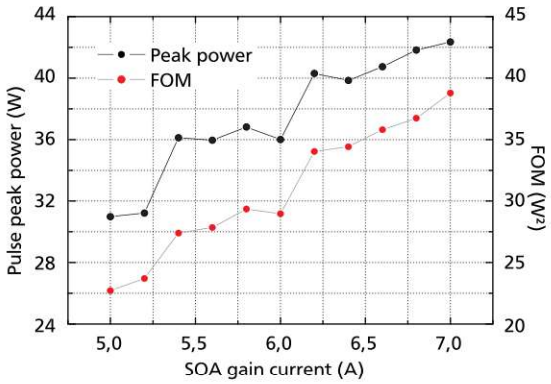

Fig. 6. Pulse peak power (left scale) and FOM (right scale) of the amplified pulses as function of the SOA gain current.

post-compression at wavelengths >1 μm thus keeping the system compact. Omitting the PSF leads to a P_{peak} of 44.7 W and a FOM of 43.6 W^2.

We have studied the amplification behavior of a tapered QD SOA at high gain currents seeded by the pulsed emission of a mode-locked tapered two-section QD laser emitting at a wavelength of 1.26 μm. A maximum pulse peak power of 42 W (44.7 W) at a pulse width of 1.37 ps is achieved leading to a FOM value of 38.5 W^2 (43.6 W^2) for TPEF applications. The numbers in brackets correspond to values obtained without the PSF.

This research was partially funded by the EU 7th Framework Program "Fast-Dot" (Grant No. 224338). S. Breuer acknowledges financial support from the Adolf-Messer-Foundation. The authors thank M. Tran, Y. Robert, and E. Vinet for excellent technical assistance.

References

1. F. Helmchen and W. Denk, Nat. Methods **2**, 932 (2005).
2. R. Aviles-Espinosa, G. Filippidis, C. Hamilton, G. Malcolm, K. J. Weingarten, T. Südmeyer, Y. Barbarin, U. Keller, S. I. Santos, D. Artigas, and P. Loza-Alvarez, Biomed. Opt. Express **2**, 739 (2011).
3. M. Kuramoto, N. Kitajima, H. Guo, Y. Furushima, M. Ikeda, and H. Yokoyama, Opt. Lett. **32**, 2726 (2007).
4. T. Ulm, F. Harth, H. Fuchs, J. A. L'Huillier, and R. Wallenstein, Appl. Phys. B **92**, 481 (2008).
5. K. Kim, S. Lee, and P. Delfyett, Opt. Express **13**, 4600 (2005).
6. C. Jördens, T. Schlauch, M. Li, M. R. Hofmann, M. Bieler, and M. Koch, Appl. Phys. B **93**, 515 (2008).
7. J. C. Balzer, T. Schlauch, A. Klehr, G. Erbert, G. Tränkle, and M. R. Hofmann, Electron. Lett. **49**, 838 (2013).
8. S. Schwertfeger, A. Klehr, T. Hoffmann, A. Liero, H. Wenzel, and G. Erbert, Appl. Opt. **52**, 3364 (2013).
9. S. Schwertfeger, A. Klehr, T. Hoffmann, A. Liero, H. Wenzel, and G. Erbert, Appl. Phys. B **103**, 603 (2011).
10. P. Adamiec, B. Bonilla, A. Consoli, J. M. G. Tijero, S. Aguilera, and I. Esquivias, Appl. Opt. **51**, 7160 (2012).
11. A. Klehr, B. Sumpf, K.-H. Hasler, J. Fricke, A. Liero, and G. Erbert, IEEE Photon. Technol. Lett. **22**, 832 (2010).
12. S. Riecke, S. Schwertfeger, K. Lauritsen, K. Paschke, R. Erdmann, and G. Tränkle, Appl. Phys. B **98**, 295 (2010).
13. E. U. Rafailov, M. A. Cataluna, and W. Sibbett, Nat. Photonics **1**, 395 (2007).
14. E. U. Rafailov, S. J. White, A. A. Lagatsky, A. Miller, W. Sibbett, D. A. Livshits, A. E. Zhukov, and V. M. Ustinov, IEEE Photon. Technol. Lett. **16**, 2439 (2004).
15. J. Yu, M. Schell, M. Schulze, and D. Bimberg, Appl. Phys. Lett. **65**, 2395 (1994).
16. M. G. Thompson, A. Rae, R. L. Sellin, C. Marinelli, R. V. Penty, I. H. White, A. R. Kovsh, S. S. Mikhrin, D. A. Livshits, and I. L. Krestnikov, Appl. Phys. Lett. **88**, 133119 (2006).
17. Y. Ding, R. Aviles-Espinosa, M. A. Cataluna, D. Nikitichev, M. Ruiz, M. Tran, Y. Robert, A. Kapsalis, H. Simos, C. Mesaritakis, T. Xu, P. Bardella, M. Rossetti, I. Krestnikov, D. Livshits, I. Montrosset, D. Syvridis, M. Krakowski, P. Loza-Alvarez, and E. Rafailov, Opt. Express **20**, 14308 (2012).
18. M. Rossetti, P. Bardella, and I. Montrosset, IEEE J. Quantum Electron. **47**, 569 (2011).
19. T. Xu, P. Bardella, M. Rossetti, and I. Montrosset, IET Optoelectron. **6**, 110 (2012).
20. D. I. Nikitichev, Y. Ding, M. A. Cataluna, E. U. Rafailov, L. Drzewietzki, S. Breuer, W. Elsaesser, M. Rossetti, P. Bardella, T. Xu, I. Montrosset, I. Krestnikov, D. Livshits, M. Ruiz, M. Tran, Y. Robert, and M. Krakowski, Laser Phys. **22**, 715 (2012).
21. P. P. Baveja, D. N. Maywar, A. M. Kaplan, and G. P. Agrawal, IEEE J. Quantum Electron. **46**, 1396 (2010).